Published in final edited form as:

Doc Ophthalmol. 2012 December ; 125(3): 203–209. doi:10.1007/s10633-012-9347-9.

Response properties of slow PIII in the *Large*^{vls} mutant

Neal S. Peachey,

Louis Stokes Cleveland VA Medical Center, 10701 East Boulevard, Cleveland, OH 44106, USA; Cole Eye Institute, Cleveland Clinic, 9500 Euclid Avenue, Cleveland, OH 44195, USA; Department of Ophthalmology, Cleveland Clinic Lerner College of Medicine of Case Western Reserve University, 9500 Euclid Avenue, Cleveland, OH 44195, USA

Gwen M. Sturgill-Short

Louis Stokes Cleveland VA Medical Center, 10701 East Boulevard, Cleveland, OH 44106, USA

Abstract

Purpose—Mouse mutants for proteins expressed in the dystrophin–glycoprotein complex at the photoreceptor terminal have electroretinogram (ERG) b-waves with a delayed onset and time course. The b-wave is defined by the sum of PII generated by depolarizing bipolar cells and slow PIII generated by Müller glial cells. In this study, we evaluated the hypothesis that the abnormalities observed in one of these mutants, *Large*^{vls}, are caused by abnormal response properties of slow PIII.

Methods—To isolate slow PIII, we crossed the *Large*^{vls} mutant to a mouse line (*Gpr179*^{nob5}) that lacks the ERG b-wave but maintains normal photoreceptor function and in which retinal degeneration does not occur. ERGs were recorded to strobe flash stimuli after overnight dark adaptation.

Results—In comparison with control responses, the a-wave and slow PIII had comparable waveforms but were reduced in amplitude in *Large*^{vls} mice. The magnitude of this reduction was comparable for these components, and across stimulus luminance. There was no stimulus condition where the amplitude of slow PIII was larger than control.

Conclusions—The data obtained are inconsistent with the idea that the b-wave abnormalities noted in *Large*^{vls} mutant mice are caused by abnormal response properties of slow PIII.

Keywords

B-wave; Electroretinogram; Müller cell; Slow PIII

Introduction

The electroretinogram (ERG) reflects the algebraic summation of several underlying generators. In response to a strobe flash presented in darkness, the ERG is comprised of two main components, the a-wave and the b-wave. The a-wave reflects the light-induced closure

neal.peachey@va.gov.

Conflict of interest None

of sodium ion channels along the rod outer segment [1]. The positive polarity b-wave reflects the summation of a positive polarity component (PII [2]) generated by rod depolarizing bipolar cells (DBCs [3]) and a negative polarity component (slow PIII) that reflects Kir4.1 channel activity in Müller glial cells induced as a secondary response to light-evoked photoreceptor activity [3-7]. These underlying generators interact to define the b-wave recorded by electrodes contacting the corneal surface. An altered b-wave could, therefore, reflect changes in PII and/or slow PIII.

An unusual ERG waveform has been reported in mutant mouse models for proteins expressed in the dystrophin-glycoprotein complex at the photoreceptor terminal, including dystrophin [8], LARGE [9, 10], pikachurin [11], and protein *O*-mannose *N*-acetylglucosaminyltransferase 1 (POMGnT1 [12]). The hallmark of these responses is a marked delay in the timing of the b-wave component, as well as amplitude reductions. These abnormalities are exemplified by the ERG waveforms shown in Fig. 1, which were evoked by a series of flashes presented to dark-adapted $Large^{+/vls}$ and $Large^{vls/vls}$ littermates. While responses of $Large^{+/vls}$ heterozygotes are comparable to those of control mice, the responses of $Large^{vls/vls}$ homozygotes have reduced a-waves and b-waves that have reduced amplitude and delayed implicit time. The basis for these response abnormalities has not been established, although they are apparent across a broad range of stimulus luminance. Pattnaik et al. [13] examined a dystrophin mutant, mdx^{Cv3}, and suggested that the abnormal b-waves noted in this model could reflect abnormal response properties of slow PIII, which together with PII defines the b-wave waveform. This suggestion was supported by in vitro studies [13] in which recordings were made from mdx^{Cv3} retinas before and after the addition of barium, an ion that blocks Kir channels and eliminates slow PIII [3]. Subtraction of these responses provides a measure of slow PIII, which was larger in mdx^{Cv3} mutant mice than in control animals. Based on these in vitro results, Pattnaik et al. [13] suggested that the abnormal waveform noted in mdx^{Cv3} mice may reflect abnormal response properties of slow PIII.

In the present study, we used a genetic approach to evaluate the hypothesis that changes in the response properties of slow PIII underlie the b-wave abnormalities observed in ERGs obtained from $Large^{vls/vls}$ mice [10]. To do this, we crossed the $Large^{vls}$ allele onto the $Gpr179^{nob5}$ line [14]. Because $Gpr179^{nob5/nob5}$ mice lack the ERG b-wave, the response properties of slow PIII can be evaluated in vivo [7, 15].

Methods

Mice

We obtained $Large^{+/vls}$ mice from The Jackson Laboratory (Bar Harbor, ME) and $Gpr179^{nob5}$ mice from a local colony. A two-generation cross was used to generate $Large^{vls/vls}$ and control ($Large^{+/vls}$ or $Large^{+/+}$) littermates that were $Gpr179^{nob5/nob5}$ homozygotes.

Genotyping

DNA was extracted from tail snips. Mice were genotyped for wild-type and mutant alleles of *Large* and *Gpr179* using PCR protocols. The *Large*^{vls} mutation arose on a Castaneous background and has been crossed to C57BL/6 J for more than 10 generations [10]. By selecting for the *Large*^{vls} allele, the only region that remains Castaneous is near that locus. We used two pairs of primers (D8MIT74, D8MIT179) for single-nucleotide polymorphisms that flank the Large locus to distinguish mice that carried Castaneous (*Large*^{vls}) or C57BL/6 J (*Large*$^{+}$) alleles. We confirmed PCR genotyping by two phenotypic features that characterize homozygotes: small stature and an epiretinal vasculature that persists into adulthood [10].

The following primers were used to screen mice for *Gpr179* alleles:

For the *Gpr179*$^{+}$ allele: sense (5′- TGTGCCTG GGTATCTGTTGA-3′)

antisense (5′- GCTTACACACTTACACACAGA- TAGATG-3′)

For the *Gpr179*^{nob5} allele: sense (5′- GCATGTGC- CAAGGGTATCTT-3′)

antisense (5′- GCTTACACACTTACACACAGA- TAGATG-3′)

ERG

After overnight dark adaptation, mice were anesthetized with ketamine (80 mg/kg) and xylazine (16 mg/kg). The cornea was anesthetized (1 % proparacaine HCl) and the pupil was dilated (2.5 % phenylephrine HCl, 1 % tropicamide, and 1 % cyclopentolate HCl). Mice were placed on a temperature-regulated heating pad throughout the recording session. All procedures involving animals were approved by the Cleveland Clinic Institutional Animal Care and Use Committee. Because the photoreceptor degeneration of *Large*$^{vls/vls}$ mice is progressive, all studies were conducted on 1-month-old mice.

Strobe flash ERGs were recorded using a stainless steel electrode in contact with the corneal surface via 1 % methylcellulose. Needle electrodes were placed in the cheek and the tail for reference and ground leads, respectively. Dark-adapted ERGs were evoked by full-field flashes (LKC Technologies, Gaithersburg, MD), with time-integrated flash luminances ranging from −3.6 to 2.1 log cd s/m^2. Stimuli were presented in order of increasing luminance and the number of successive responses averaged together decreased from 20 for low-luminance flashes to 2 for the highest luminance stimuli. The duration of the interstimulus interval increased from 4 s for low-luminance flashes to 90 s for the highest luminance stimuli. Responses were differentially amplified (0.3–1,500 Hz), averaged, and stored using a UTAS E-3000 signal averaging system (LKC Technologies, Gaithersburg, MD).

The amplitude of the a-wave was measured at 8 ms after flash presentation from the pre-stimulus baseline. The amplitude of slow PIII was measured from the pre-stimulus baseline to the value of the trough at 150 ms after flash presentation.

Results

Figure 2 illustrates the expected results if changes in the response properties of slow PIII cause the b-wave abnormalities observed in ERGs obtained from *Large*$^{vls/vls}$ mice. Response (1) re-plots the *Large*$^{+/vls}$ response to a 0.0 log cd s/m^2 stimulus from Fig. 1. Response (2) is the response of a *Gpr179*$^{nob5/nob5}$ mouse to the same stimulus. The absence of the b-wave in the *Gpr179*$^{nob5/nob5}$ mouse response allows slow PIII to be measured. Responses (1) and (2) have been normalized at 24 ms. Response (3) is the result of subtracting response (2) from response (1). This difference waveform reflects all of the ERG components that are missing in the responses of *Gpr179*$^{nob5/nob5}$ mice and resembles the PII component extracted by others using curve-fitting or pharmacological approaches [16, 17]. Response (4) re-plots from Fig. 1 the *Large*$^{vls/vls}$ mutant response to a 0.0 log cd s/m^2 stimulus. Response (4) was normalized in the same manner as responses (1) and (2). Working from the presumption that the *Large*$^{vls/vls}$ mutant PII component generated by DBCs has a normal waveform, we subtracted response (3) from response (4) to derive the predicted *Large*$^{vls/vls}$ mutant PIII component. This is shown as response (5) and is seen to be substantially larger in amplitude than the corresponding component obtained from control *Gpr179*$^{nob5/nob5}$ mice [response (2)]. If abnormal slow PIII response properties underlie the abnormal *Large*^{vls} b-wave, we expect to see a similar slow PIII phenotype in *Large*$^{vls/vls}$/*Gpr179*$^{nob5/nob5}$ double mutant mice.

Figure 3 presents a series of dark-adapted ERGs obtained from *Large*$^{+/+}$ (left) and *Large*$^{vls/vls}$ mutant (right) littermates. Because both mice are *Gpr179*$^{nob5/nob5}$ homozygotes, the b-wave is eliminated and slow PIII is revealed. At low stimulus luminances, the response is comprised of a small negative polarity deflection. At high stimulus luminances, the a-wave becomes apparent ahead of slow PIII. The response of the *Large*$^{vls/vls}$ mutant has a waveform that resembles that of the control, but is reduced in amplitude.

Figure 4 presents luminance-response functions for the a-wave (A) and for slow PIII (B). In comparison with control, both response components are reduced in *Large*$^{vls/vls}$ mutants. To determine whether the magnitude of reductions in a-wave and slow PIII amplitude are comparable, at each flash luminance the average mutant response was divided by the corresponding control average. Across the stimulus range used here, the *Large*$^{vls/vls}$ responses are 55 ± 1.5 (a-wave) and 55.7 ± 2.9 % (slow PIII) of control. These values are not significantly different from one another ($t < 1$), indicating that the a-wave and slow PIII are reduced by equivalent amount in *Large*$^{vls/vls}$ mice.

The *Large*$^{vls/vls}$/*Gpr179*$^{nob5/nob5}$ responses do not resemble the waveforms predicted (response (5), Fig. 2) if the PII component of *Large*$^{vls/vls}$ ERGs had a normal waveform and the abnormal response was due to changes in the response properties of slow PIII. There was no stimulus condition in which the amplitude of slow PIII was larger in *Large*$^{vls/vls}$ than control mice.

To define the *Large*$^{vls/vls}$ PII waveform, we subtracted *Gpr179*$^{nob5/nob5}$ ERG from *Gpr179*$^{+/+}$ responses, obtained to 1.4 log cd s/m^2 stimulus flashes. In Fig. 5, response (1) plots a *Large*$^{+/vls}$ *Gpr179*$^{+/+}$ ERG and response (2) is the ERG of a *Large*$^{+/vls}$/

Gpr179$^{nob5/nob5}$ mouse. These waveforms were normalized at 8 ms. Response (3) is the result of subtracting response (2) from response (1) and reflects the normal PII component obtained under this stimulus condition. Response (4) plots a*Large*$^{vls/vls}$/*Gpr179*$^{+/+}$ ERG and response (5) is the ERG of a *Large*$^{vls/vls}$/*Gpr179*$^{nob5/nob5}$ mouse; these waveforms were also normalized at 8 ms. Response (6) is the result of subtracting response (5) from response (4) and represents the *Large*$^{vls/vls}$ PII component with response (3) re-plotted as the dashed line. The superimposition of the difference waveforms shows that in comparison with the control, the *Large*$^{vls/vls}$ PII component is delayed and has a reduced amplitude.

Discussion

In the present study, we have examined the in vivo response properties of slow PIII to evaluate the possibility that abnormal response properties of this ERG component underlie the b-wave abnormalities observed in *Large*$^{vls/vls}$ mutant mice. We isolated slow PIII genetically, by crossing the *Large*$^{vls/vls}$ mutant to a mouse line that does not generate a b-wave due to a *Gpr179* null mutation [14]. While the *Gpr179*$^{nob5/nob5}$ mutant does not generate a b-wave, the retina appears normal by light and electron microscopy [14]. The main abnormality noted in double mutant *Large*$^{vls/vls}$/*Gpr179*$^{nob5/nob5}$ mice is an overall reduction in slow PIII amplitude that is proportional to the amplitude reduction noted for the a-wave. Samuels et al. [15] reported a similar analysis of *Prph*$^{Rd2/+}$/*Nyx*^{nob} mice and noted that the amplitude of slow PIII was somewhat larger than predicted by the a-wave reduction. Periphe-rin/rds is an outer segment protein [15,18], and *Prph*$^{Rd2/+}$ mice do not display the b-wave abnormalities noted in *Large*$^{vls/vls}$ mice [19]. If we take these results as a benchmark, the amplitude reductions noted in slow PIII of the *Large*$^{vls/vls}$ mutant are somewhat greater than expected based on the a-wave loss and inconsistent with the idea that an abnormally large amplitude slow PIII underlies the b-wave abnormalities noted in this mutant.

These findings do not rule out the possibility that an increase in slow PIII could contribute to the b-wave abnormalities noted in other mutants, including the *mdx*^{Cv3} mouse. We chose to examine the *Large*^{vls} mutant based on our prior experience [10]. It would be interesting to address this possibility in vivo by crossing the *mdx*^{Cv3} mutant to the *Gpr179*^{nob5} mutant or any of the other no b-wave mutants that have been described for *Nyx* [20, 21], *Grm6* [22-24], and *Trpm1* [25-28].

While the present results indicate that slow PIII abnormalities do not underlie the delayed onset and slow kinetics of the *Large*^{vls} b-wave (Fig. 1), they do not provide an explanation for these abnormalities. A recent study of the *Pikachurin*$^{-/-}$ mouse, which has ERG abnormalities comparable to those of *Large*$^{vls/vls}$, indicates that DBC invaginations into photoreceptor terminals are abnormal, resulting in a larger gap between the pre-synaptic active zone and the post-synaptic membrane [29]. A larger synaptic gap could delay clearance of glutamate and thus result in a delayed b-wave. It remains to be determined whether the synaptic abnormalities present in *Large*$^{vls/vls}$ mice [10] include this feature.

Acknowledgments

This research was supported by the US Veterans Administration Medical Research Service, a Foundation Fighting Blindness Center Grant to the Cole Eye Institute, Cleveland Clinic, and an unrestricted award from Research to Prevent Blindness to the Department of Ophthalmology, Cleveland Clinic Lerner College of Medicine.

References

1. Penn RD, Hagins WA (1969) Signal transmission along retinal rods and the origin of the electroretinographic a-wave. Nature 223:201–204 [PubMed: 4307228]
2. Granit R (1933) The components of the retinal action potential in mammals and their relation to the discharge in the optic nerve. J Physiol 77:207–239 [PubMed: 16994385]
3. Kofuji P, Ceelen P, Zahs KR, Surbeck LW, Lester HA, Newman EA (2000) Genetic inactivation of an inwardly rectifying potassium channel (Kir4.1 subunit) in mice: phenotypic impact in retina. J Neurosci 20:5733–5740 [PubMed: 10908613]
4. Steinberg RH, Miller S (1973) Aspects of electrolyte transport in frog pigment epithelium. Exp Eye Res 16:365–372 [PubMed: 4542605]
5. Oakley B II, Green DG (1976) Correlation of light-induced changes in retinal extracellular potassium concentration with c-wave of the electroretinogram. J Neurophysiol 39: 1117–1133 [PubMed: 1086346]
6. Witkovsky P, Dudek FE, Ripps H (1975) Slow PIII component of the carp electroretinogram. J Gen Physiol 65:119–134 [PubMed: 1117278]
7. Wu J, Marmorstein AD, Kofuji P, Peachey NS (2004) Contribution of Kir4.1 to the mouse electroretinogram. Mol Vision 10:650–654
8. Pillers DA (1999) Dystrophin and the retina. Mol Genet Metab 68:304–309 [PubMed: 10527681]
9. Holzfeind PJ, Grewal PK, Reitsamer HE, Kechvar J, Lass-mann H, Hoeger H, Hewitt JE, Bittner RE (2002) Skeletal, cardiac and tongue muscle pathology, defective retinal transmission, and neuronal migration defects in the *Large*^{myd} mouse defines a natural model for glycosylation-deficient muscle-eye-brain disorders. Hum Mol Genet 11: 2673–2687 [PubMed: 12354792]
10. Lee Y, Kameya S, Cox GA, Hsu J, Hicks W, Maddatu TP, Smith RS, Naggert JK, Peachey NS, Nishina PM (2005) Ocular abnormalities in *Large*^{myd}and *Large*^{vls} mice, spontaneous models for muscle, eye and brain diseases. Mol Cell Neurosci 30:160–172 [PubMed: 16111892]
11. Sato S, Omori Y, Katoh K, Kondo M, Kanagawa M, Miyata K, Funabiki K, Koyasu T, Kajimura N, Miyoshi T, Sawai H, Kobayashi K, Tani A, Toda T, Usukura J, Tano Y, Fujikado T, Furukawa T (2008) Pikachurin, a dystroglycan ligand, is essential for photoreceptor ribbon synapse formation. Nat Neurosci 11:923–931 [PubMed: 18641643]
12. Liu J, Ball SL, Yang Y, Mei P, Zhang L, Shi H, Kaminski HJ, Lemmon VP, Hu H (2006) A genetic model for muscle-eye-brain disease in mice lacking protein O-mannose beta1,2-*N*-acetylglucosaminyltransferase (POMGnT1). Mech Dev 123:228–240 [PubMed: 16458488]
13. Pattnaik BR, Green DG, Pillers D-AM (2009) Aberrant slow wave (Slow PIII) component superimposed on a normal b-wave, accounts for the abnormal electroretinogram in the *mdx*^{Cv3} mouse. Invest Ophthalmol Vis Sci 50:E-Abstract 3599
14. Peachey NS, Ray TA, Florijn R, Rowe LB, Sjoerdsma T, Contreras-Alcantara S, Baba K, Tosini G, Pozdeyev N, Iuvone PM, Bojang P Jr, Pearring JN, Simonsz HJ, van Genderen M, Birch DG, Traboulsi EI, Dorfman A, Lopez I, Ren H, Goldberg AFX, Nishina PM, Lachapelle P, McCall MA, Koenekoop RK, Bergen AAB, Kamermans M, Gregg RG (2012) GPR179 is required for depolarizing bipolar cell function and is mutated in autosomal-recessive complete congenital stationary night blindness. Am J Hum Genet 90:331–339 [PubMed: 22325362]
15. Samuels IS, Sturgill GM, Grossman GH, Rayborn ME, Hollyfield JG, Peachey NS (2010) Light-evoked responses of the retinal pigment epithelium: changes accompanying photoreceptor loss in the mouse. J Neurophysiol 104: 391–402 [PubMed: 20484527]
16. Hood DC, Birch DG (1992) A computational model of the amplitude and implicit time of the b-wave of the human ERG. Vis Neurosci 8:107–126 [PubMed: 1558823]

17. Robson JG, Frishman LJ (1995) Response linearity and kinetics of the cat electroretinogram: the bipolar cell component of the dark-adapted electroretinogram. Vis Neurosci 12:837–850 [PubMed: 8924408]

18. Goldberg AF (2006) Role of peripherin/rds in vertebrate photoreceptor architecture and inherited retinal degenerations. Int Rev Cytol 253:131–175 [PubMed: 17098056]

19. Cheng T, Peachey NS, Li S, Goto Y, Cao Y, Naash MI (1997) The effect of peripherin/rds haploinsufficiency on rod and cone photoreceptors. J Neurosci 17:8118–8128 [PubMed: 9334387]

20. Pardue MT, McCall MA, LaVail MM, Gregg RG, Peachey NS (1998) A naturally-occurring mouse model of X-linked congenital stationary night blindness. Invest Ophthalmol Vis Sci 39:2443–2449 [PubMed: 9804152]

21. Gregg RG, Kamermans M, Klooster J, Lukasiewicz PD, Peachey NS, Vessey KA, McCall MA (2007) Nyctalopin expression in retinal bipolar cells restores visual function in a mouse model of complete X-linked congenital stationary night blindness. J Neurophysiol 98:3023–3033 [PubMed: 17881478]

22. Masu M, Iwakabe H, Tagawa Y, Miyoshi T, Yamashita M, Fukuda Y, Sasaki H, Hiroi K, Nakamura Y, Shigemoto R, Takada M, Nakamura K, Nakao K, Katsuki M, Nakanishi S (1995) Specific deficit of the ON response in visual transmission by targeted disruption of the mGIuR6 gene. Cell 80:757–765 [PubMed: 7889569]

23. Pinto LH, Vitaterna MH, Shimomura K, Siepka SM, Bal-annik V, McDearmon EL, Omura C, Lumayag S, Invergo BM, Glawe B, Cantrell DR, Inayat S, Olvera MA, Vessey KA, McCall MA, Maddox D, Morgans CW, Young B, Pletcher MT, Mullins RF, Troy JB, Takahashi JS (2007) Generation, identification and functional characterization of the *nob4* mutation of *Grm6* in the mouse. Vis Neurosci 24:111–123 [PubMed: 17430614]

24. Maddox DM, Vessey KA, Yarbrough GL, Invergo BM, Cantrell DR, Inayat S, Balannik V, Hicks WL, Hawes NL, Byers S, Smith RS, Hurd R, Howell D, Gregg RG, Chang B, Naggert JK, Troy JB, Pinto LH, Nishina PM, McCall MA (2008) Allelic variance between *GRM6* mutants, $Grm6^{nob3}$ and $Grm6^{nob4}$ results in differences in retinal ganglion cell visual responses. J Physiol 586: 4409–4424 [PubMed: 18687716]

25. Morgans CW, Zhang J, Jeffrey BG, Nelson SM, Burke NS, Duvoisin RM, Brown RL (2009) TRPM1 is required for the depolarizing light response in retinal ON-bipolar cells. Proc Natl Acad Sci USA 106:19174–19178 [PubMed: 19861548]

26. Shen Y, Heimel JA, Kammermans M, Peachey NS, Gregg RG, Nawy S (2009) A transient receptor potential-like channel mediates synaptic transmission in rod bipolar cells. J Neurosci 29:6088–6093 [PubMed: 19439586]

27. Koike C, Obara T, Uriu Y, Numata T, Sanuki R, Miyata K, Koyasu T, Ueno S, Funabiki K, Tani A, Ueda H, Kondo M, Mori Y, Tachibana M, Furukawa T (2010) TRPM1 is a component of the retinal ON bipolar cell transduction channel in the mGluR6 cascade. Proc Natl Acad Sci USA 107:332–337 [PubMed: 19966281]

28. Peachey NS, McCall MA, Nobles RD, Hirschtritt ME, Pearring JN, Bojang P, Shen Y, Nawy SA, Nishina PM, Gregg RG (2011) *Trpml* point mutation underlies retinal dysfunction in the *Mtvr27* mouse model of complete congenital stationary night blindness. Invest Ophthalmol Vis Sci 51:E-Abstract 4124

29. Omori Y, Araki F, Chaya T, Kajimura N, Irie S, Terada K, Muranishi Y, Tsujii T, Ueno S, Koyasu T, Tamaki Y, Kondo M, Amano S, Furukawa T (2012) Presynaptic dystroglycan-pikachurin complex regulates the proper synaptic connection between retinal photoreceptor and bipolar cells. J Neurosci 32:6126–6137 [PubMed: 22553019]

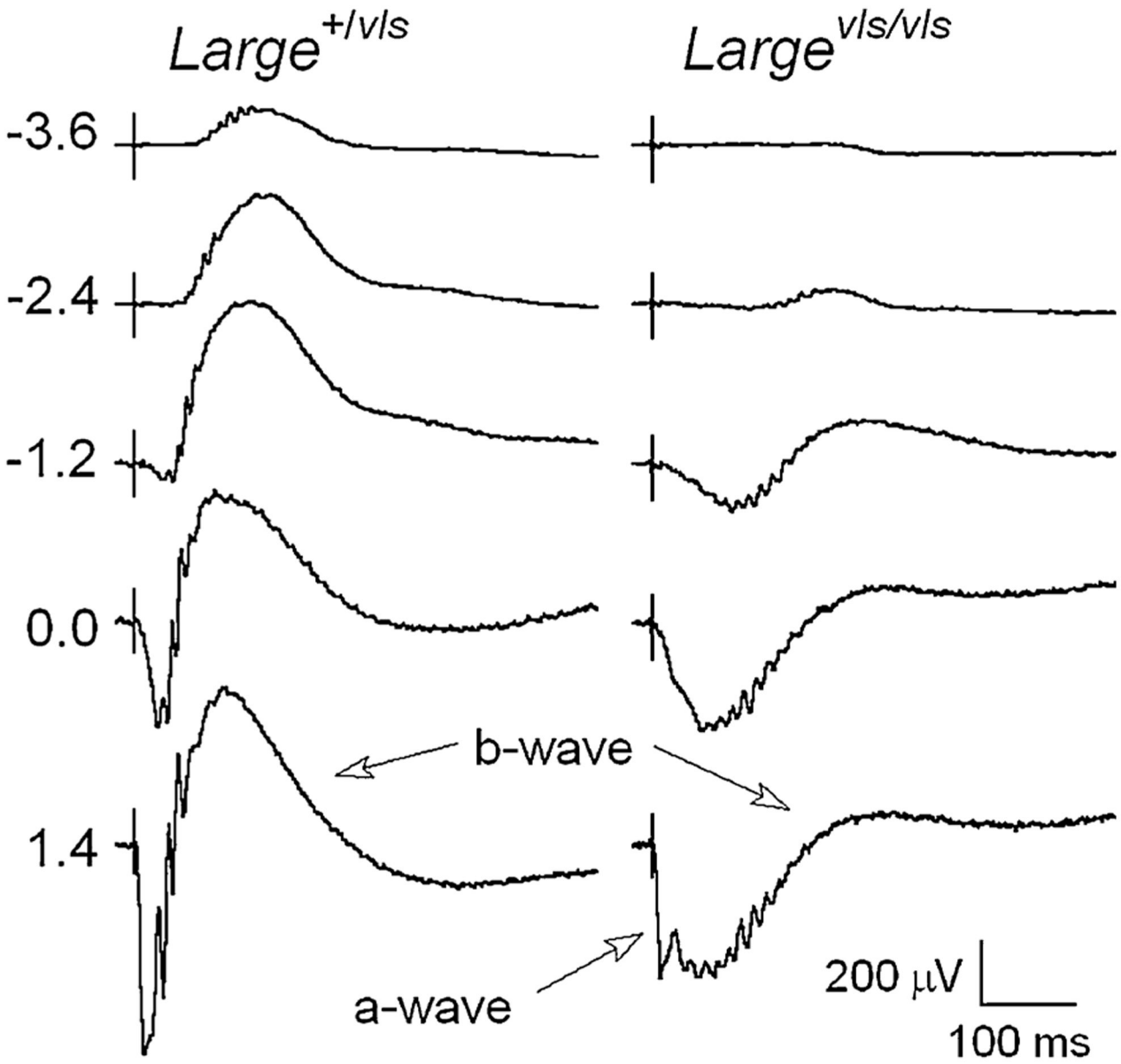

Fig. 1.

Comparison of dark-adapted ERGs obtained from *Large*$^{+/vls}$ and *Large*$^{vls/vls>}$ mice. Values to the left of each row of waveforms indicate flash luminance in log cd s/m^2

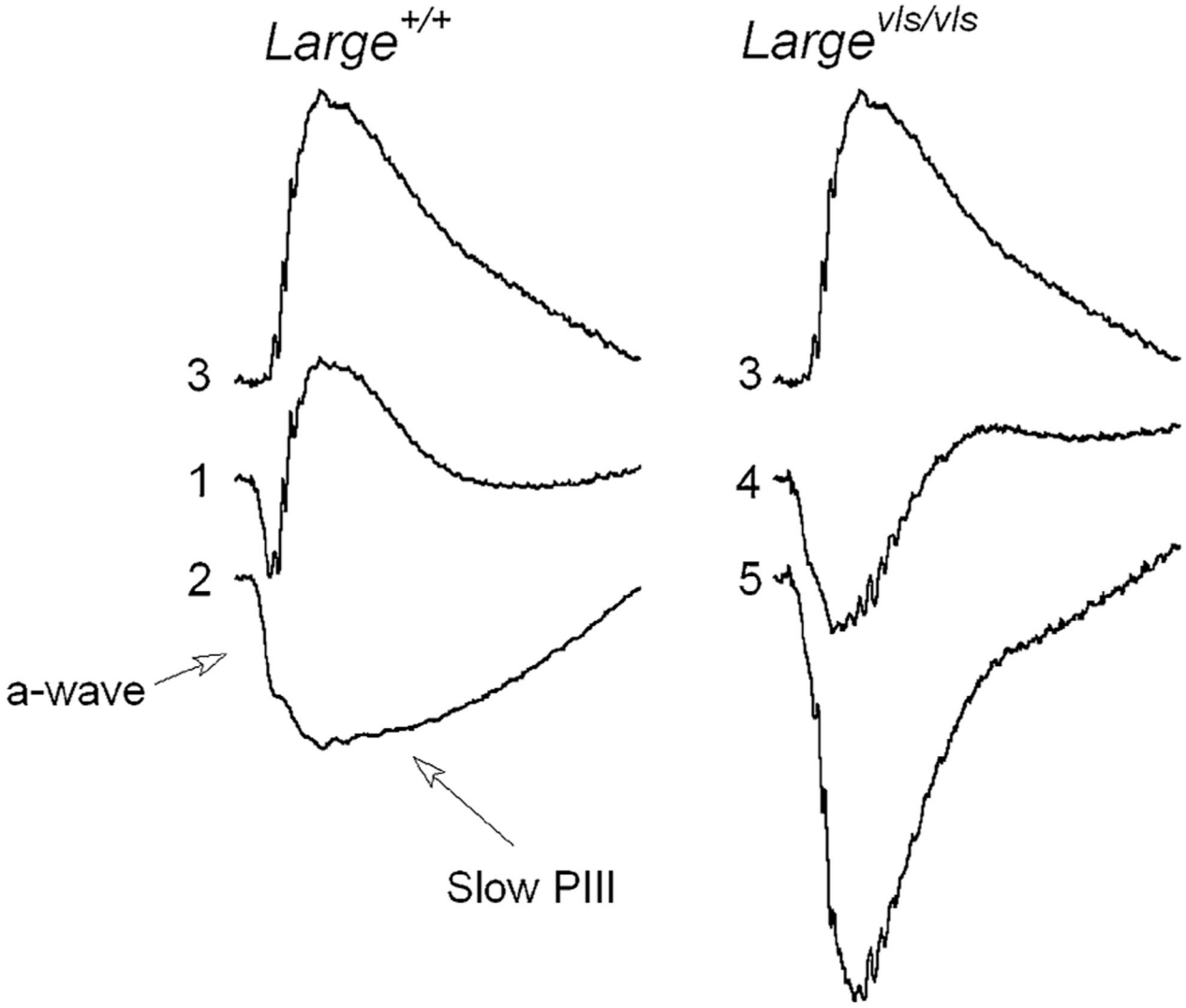

Fig. 2.

Predicted result if changes in response properties of slow PIII underlie abnormal *Large*^{vls} ERG waveform. Responses (1) and (2) were evoked by 0.0 log cd s/m^2 stimulus flashes from control (1) and *Gpr179*$^{nob5/nob5}$ (2) mice. Response (3) represents the result of subtracting response (2) from response (1). Response (4) was evoked by 0.0 log cd s/m^2 stimuli from a *Large*$^{vls/vls}$ mouse. Response (5) indicates the result of subtracting response (3) from response (4) and represents the waveform expected if *Large*$^{vls/vls}$ ERGs include a normal waveform P2 component. All responses are normalized to a-wave at 24 ms, corresponding to the trough of response (1)

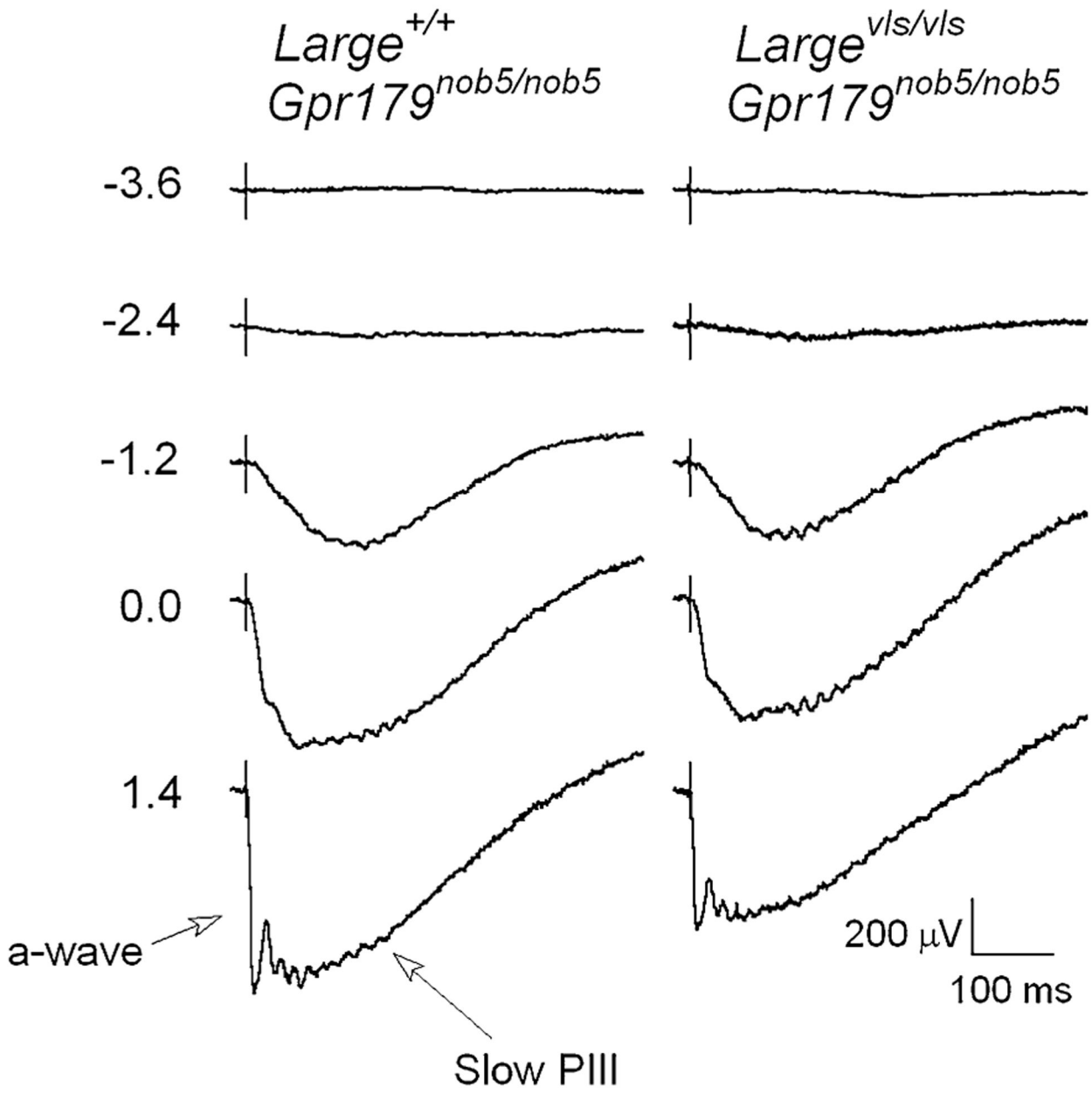

Fig. 3.

Comparison of dark-adapted ERGs obtained from *Large*$^{vls/vls}$/*Gpr179*$^{nob5/nob5}$ and *Large*$^{+/+}$/*Gpr179*$^{nob5/nob5}$ mice. Values to the left of each row of waveforms indicate flash luminance in log cd s/m^2

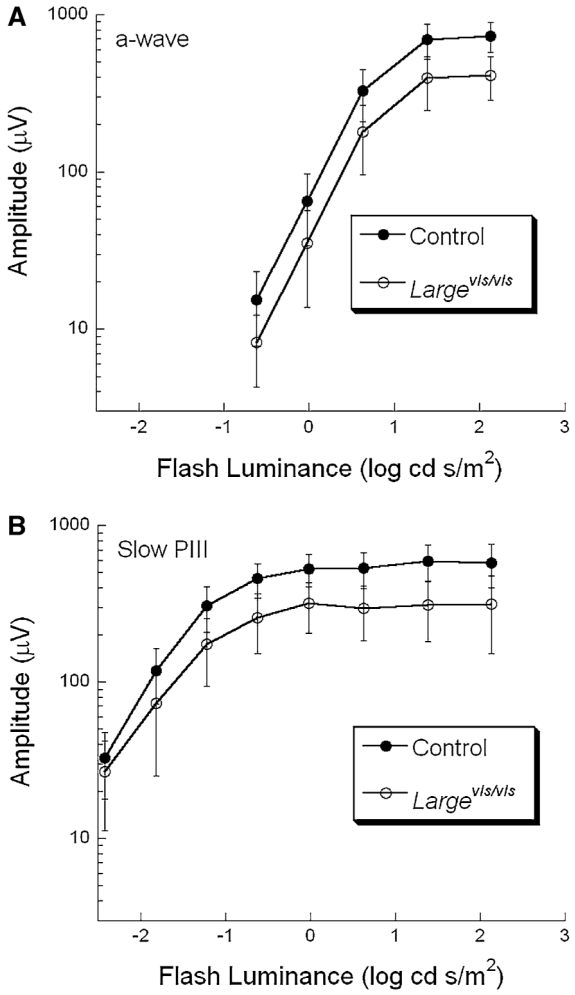

Fig. 4.

Response functions for the ERG a-wave (A) and slow PIII (B) measures of *Large*$^{vls/vls}$/*Gpr179*$^{nob5/nob5}$ and control/*Gpr179*$^{nob5/nob5}$ mice. Data points indicate the average (± s.d.) of 7 *Large*$^{vls/vls}$/*Gpr179*$^{nob5/nob5}$ and 18 control/*Gpr179*$^{nob5/nob5}$ mice

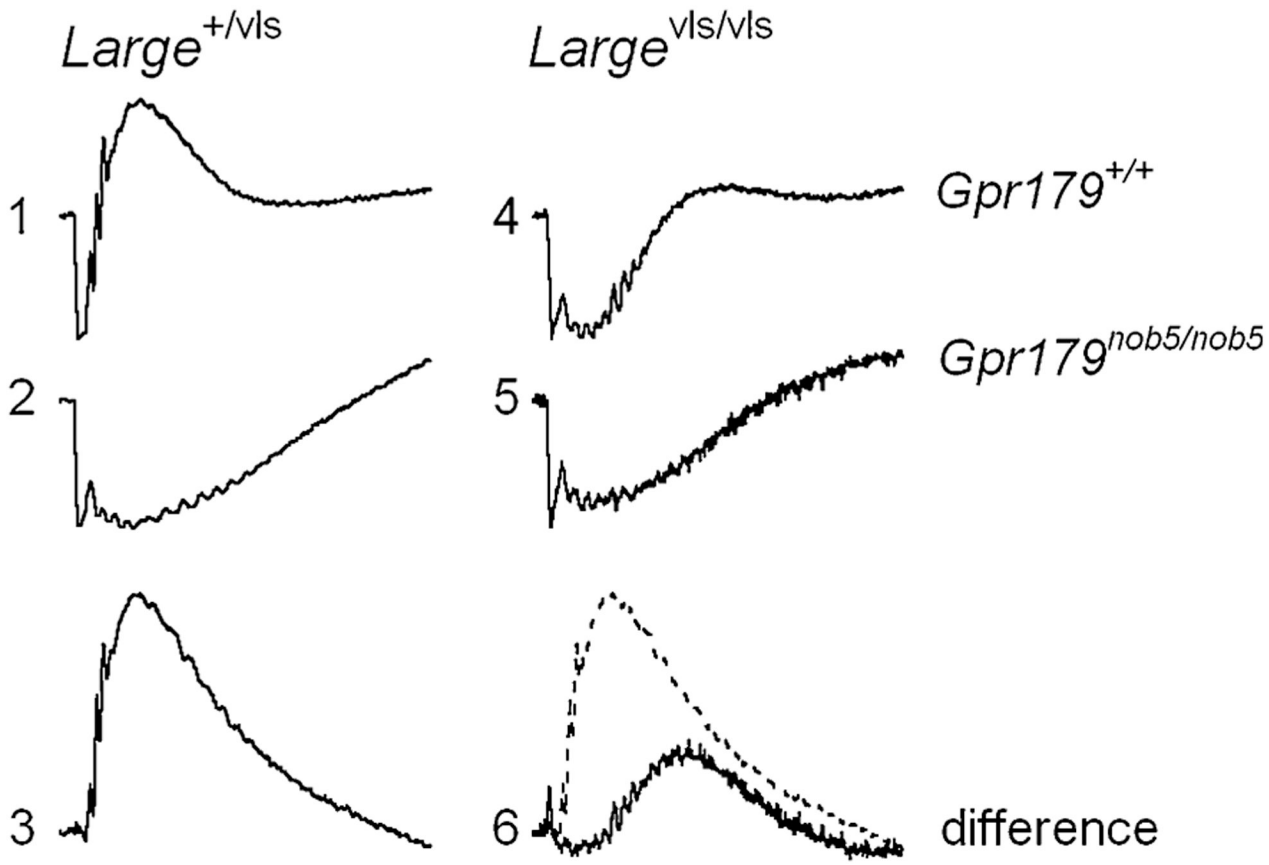

Fig. 5.

Isolation of PII from *Large*$^{+/vls}$ and *Large*$^{vls/vls}$ ERGs. ERGs evoked by 1.4 log cd s/m^2 stimulus flashes from *Large*$^{+/vls}$ (1, 2) and *Large*$^{vls/vls}$ (4, 5) mice. All responses were normalized at 8 ms. Response (3) was obtained by subtracting response (2) from response (1); response (6) was obtained by subtracting response (5) from response (4). The dashed line superimposed on response (6) is response (3)